Uppsala University
Signals and Systems

A SIGNAL PROCESSING APPROACH TO PRACTICAL NEUROPHYSIOLOGY

A Search for Improved Methods in Clinical Routine and Research

Björn Hammarberg

UPPSALA UNIVERSITY 2002

Dissertation for the degree of Doctor of Philosophy
in Signal Processing at Uppsala University, 2002

ABSTRACT

Hammarberg, B., 2002. A Signal Processing Approach to Practical Neurophysiology: A Search for Improved Methods in Clinical Routine and Research, 222 pp. Uppsala. ISBN 91-506-1551-3.

Signal processing within the neurophysiological field is challenging and requires short processing time and reliable results. In this thesis, three main problems are considered.

First, a modified line source model for simulation of muscle action potentials (APs) is presented. It is formulated in continuous-time as a convolution of a muscle-fiber dependent transmembrane current and an electrode dependent weighting (impedance) function. In the discretization of the model, the Nyquist criterion is addressed. By applying anti-aliasing filtering, it is possible to decrease the discretization frequency while retaining the accuracy. Finite length muscle fibers are incorporated in the model through a simple transformation of the weighting function. The presented model is suitable for modeling large motor units.

Second, the possibility of discerning the individual AP components of the concentric needle electromyogram (EMG) is explored. Simulated motor unit APs (MUAPs) are prefiltered using Wiener filtering. The mean fiber concentration (MFC) and jitter are estimated from the prefiltered MUAPs. The results indicate that the assessment of the MFC may well benefit from the presented approach and that the jitter may be estimated from the concentric needle EMG with an accuracy comparable with traditional single fiber EMG.

Third, automatic, rather than manual, detection and discrimination of recorded C-fiber APs is addressed. The algorithm, detects the APs reliably using a matched filter. Then, the detected APs are discriminated using multiple hypothesis tracking combined with Kalman filtering which identifies the APs originating from the same C-fiber. To improve the performance, an amplitude estimate is incorporated into the tracking algorithm. Several years of use show that the performance of the algorithm is excellent with minimal need for audit.

Keywords: matched filter, asynchronous detection, Kalman filter, initialization, MHT, Wiener deconvolution, line source model, electromyography, needle EMG, motor unit potential, MUAP, mean fiber concentration, jitter, microneurography, C-fiber, spike sorting

Björn Hammarberg, Signals and Systems, Uppsala University, PO Box 528, SE-751 20 Uppsala, Sweden. Email: Bjorn.Hammarberg@signal.uu.se.

ISBN 91-506-1551-3
Printed in Sweden by Elanders Gotab AB, Stockholm 2002
Distributed by Signals and Systems, Uppsala University, Uppsala, Sweden

To everyone who finds it useful

CONTENTS

LIST OF TABLES

The answer is out there, Neo.
It's looking for you and it will find you,
if you want it to.

Trinity, in *The Matrix*.

Preface and acknowledgments

My main purpose when setting out on this journey six years ago was to develop algorithms that may actually be used in practice. Consequently, the applications presented herein are tailored to work reliably in a practical situation and, when being in conflict, optimality has been traded for applicability.

From time to time, challenging obstacles have crossed my path and I have often asked myself if this really was what I wanted. Obviously, I have been able to surmount the barriers sufficiently often, and in retrospect, I may proudly notice that things have worked out remarkably well.

Hopefully, this work may contribute in making this world a slightly better place; not necessarily for mankind but maybe in the everyday life of the physician examinating his patient, the patient being diagnosed, the researcher analyzing his experiments, or the engineer challenged with a signal processing problem.

Regarding the thesis, it is intended for readers ranging from an engineer with a biomedical interest to a physician interested in engineering. To comply with this intention, I have put an effort in providing background information both from medicine and engineering.

To facilitate the applicability of the algorithms presented, I have as far as possible provided all details and reasonings necessary to re-implement and apply the algorithms in reality. In the literature, this type of information is often omitted which may cause a lot of frustration.

The thesis consists of two main portions of which the second part, the applications, makes up the main contribution of this work. The first part provides the signal processing foundation on which the applications are built. Hence, the knowledgeable reader, familiar with the signal processing concepts presented therein, may benefit the most from using it as a reference.

The introduction of the thesis provides a comprehensive overview that is primarily intended for persons non-familiar with neurophysiology. It provides the basic knowledge needed to fully appreciate the rest.

Several persons have had a part in this work. First of all, I would like to express my deepest gratitude to my supervisors Anders Ahlén, Mikael Sternad, Erik Stålberg, and Erik Torebjörk for their unconditional support and tutorship during these years.

There are also a number of people without whom I probably wouldn't have done this at all. I hereby gratefully acknowledge: Lars Antoni, who advised me to call Erik Stålberg and apply for a job; Karin Rouleveld, for introducing me to her supervisor; Dick Stegeman, for arranging a job for me at his department in Nijmegen; all his staff for providing an excellent atmosphere; and especially, the PhD students who thrilled me to become a PhD student myself upon coming home.

During the course as a research engineer and, in time, a PhD student I have learnt to know many wonderful persons. I would like to thank all my colleagues at the Department of Clinical Neurophysiology for providing such a friendly and supportive environment. I especially mention the other engineers Peo Fällmar, Lars Karlsson, Stefan Stålberg, David Ullström, Per Ytterberg, and Mats Åström for all enjoyable moments at work and at the traditional Svenssons events. Special thanks goes to David who helped me with one of the images in the introduction.

I would like to acknowledge Lena Eriksson and Maggan Grindlund for always being so cheerful. Many thanks to Lena for providing me with EMG signals.

I express my gratitude towards Clemens Forster, Martin Schmelz, Christian Weidner, and all the others at the Erlangen lab for great company and partnership.

I thank all my colleagues at the Signals and Systems group for all memorable moments and events. Thanks goes to the other PhD students and especially my roommates Torbjörn Ekman and Nilo Casimiro-Ericsson. Special thanks goes to Claes Tidestav for all invaluable help with various LaTeX issues, to Jonas Öhr for being who he his and for all interesting discussions, and Ove Ewerlid for providing me with the basic linux setup and teaching me how to improve it further.

Anders Svärdström deserves a special acknowledgment for his extensive experience in putting theory into practice and for his invaluable help in this regard.

Most importantly, I would like to thank my wonderful wife Anna-Carin for your love and support. You have been completely invaluable and the most important reason for my success. Thank you for your excellent help with proofreading the manuscript. Moreover, you deserve a special acknowledgment for taking care of all things I have neglected the last several weeks.

Finally, I thank my precious and joyful son Fredrik for all unforgettable moments you give; I have really missed your company during this busy time. With this put to an end, I am looking forward to all the time we will spend together.

Björn Hammarberg
Uppsala, 19 March 2002.

CHAPTER 1

Introduction

UNDERSTANDING how nerve and muscle cells work is an ancient interest. There are written records from 1700 B.C. that claims to be a transcription of an even older document describing a thorough neurophysiological case study [18] [31]. Modern neurophysiology, however, did not begin to formalize until Luigi Galvani, around 1780-1790 A.D., caused the famous twitches of a frog leg during a dissection. He discovered that the twiches were provoked by touching the nerve of the leg with a metal knife.

Upon trying to explain Galvanis observation, Alessandro Volta had discovered that a current (later known as a Galvanic current) is induced if two metal plates are connected via an electrolytic medium.[1] Based on this finding, Volta stated in 1792 that the twitches in the frog leg were provoked by an electrical current between the steel knife and the tin plate upon which the leg was lying. Later experiments proved Volta right.

This was the beginning of an important paradigm shift that established the base of modern neurophysiology. Prior to Galvani's discovery, Descartes and others claimed that the nerves were hollow tubes carrying "vital spirits" but now it was clear that the nerves were electrical conductors of some kind. Further experiments showed that even the muscles had many similarities with the nerves in this respect.

Progressively, new discoveries adding to the knowledge of the functions of muscles and nerves were being made. Due to technical difficulties, however, most advances during the 19th century were on the anatomical level. The mystery of whether the nerves were similar to metal wire conductors or whether the situation was more complex remained.

[1] This discovery was later used by Volta to invent the first electric battery, the Voltaic pile.

Owing to instrumentation improvements, measurements that provided new insights became possible to carry out and, as the end of the 19th century was approaching, the functional knowledge of nerves and muscles increased rapidly. To mention a few achievements, Hermann von Helmholtz was in 1852 able to measure the conduction velocity of a nerve signal, realizing it was much too small to be explained by simple conduction as in a metal wire.

Further indications along this line was obtained when Sidney Ringer around 1880 discovered that in order for an isolated frog heart to continue beating, salts needed to be present in the surrounding solution. Specifically, sodium (Na), calcium (Ca), and potassium (K) salts were needed and had to be in special concentrations relative to each other.

A clear hypothesis for the conduction of the nerve signal was not available until Julius Bernstein in 1902 proposed that the inactive nerve or muscle fiber is normally electrically polarized (negative inside) and that the *action potential* (AP), as he called it, is a self perpetuating depolarization and repolarization of the cell membrane. He also made the first real theoretical contribution in assuming a semipermeable cell membrane that could help explain the resting potential through differences in potassium ion (K+) concentrations on the inside and outside of nerve and muscle cells.

With the invention of the cathode ray oscilloscope in 1897, the measurements were significantly improved, both in accuracy and in feasibility. In 1913, the Nobel Prize winner, Edgar Douglas Adrian determined that the signal being transmitted is pulse-code modulated, i.e., rather than being conducted as continuous signals, the information is conducted as pulses in all-or-nothing responses with the pulse repetition frequency proportional to the strength of the signal.

1.1 The constitution and function of nerves

One of the most annoying and irrefutable findings against the hollow-nerve theory of Descartes was the repeated anatomical reports of nerves actually being anything but hollow. Further anatomical studies revealed that the nerve trunks are actually constituted by nerve fibers, or *axons*. These are responsible for conducting the AP from the nerve cell body to its destination at the *nerve terminal*, see Figure 1.1. The input to the cell is acquired through the so-called *dendrites*. With these and other findings, a profound neurophysiological knowledge of the nerves was beginning to formalize.

Still, the key principle behind the nerve conduction was unknown. To get further knowledge of the electrochemical events taking place in the nerve cell during the AP conduction, John Z. Young was in 1937 one of the first to make use of the

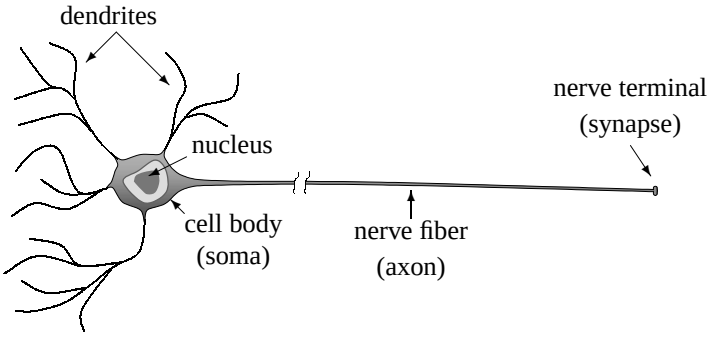

Figure 1.1: A nerve cell with the most important parts indicated.

giant axon in squid. This axon has a diameter of about 0.8 mm which is approximately 100 to 1000 times larger than other animal neurons; hence the attribute "giant".

The ease of working with large neurons made important experiments possible for the first time. This included the first intracellular recordings of the nerve cell AP as well as the first measurements of the underlying ionic currents which produce them.

1.1.1 The electrical properties of the cell membrane

Around 1940, Alan L. Hodgkin together with Andrew F. Huxley and, independently, Kenneth S. Cole along with H. J. Curtis made the first measurements of the actual membrane voltage during an AP. The results were somewhat unexpected. From Bernstein's hypothesis, the membrane voltage was anticipated to increase from its negative value about -65 mV to zero during the depolarization of the membrane. Instead, the potential continued to increase and peaked near +50 mV.

It was suggested that this observation might arise from the membrane becoming selectively permeable to sodium ions (Na^+) and this was later confirmed by Hodgkin and Katz in 1949.

To explain why the permeability of specific ions and the peak value of the membrane voltage are important factors, we note that there are two forces which act on the ions over the membrane, see Figure 1.2. First, if the *concentration* of a certain ion is different on the two sides of the membrane, this *concentration gradient* asserts a force on the ion towards the side with the *lowest* concentration to level out the difference. Second, if the *potential* is different on the two sides of the membrane, this *voltage gradient* asserts a force on a positive ion towards the side with *negative* potential and vice versa for negative ions.

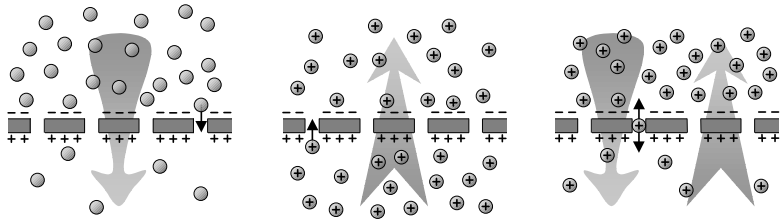

(a) (b) (c)

Figure 1.2: The effect on particles of concentration and voltage gradients over a cell membrane. In all diagrams, the compartment above the membrane has a lower potential than the compartment below the membrane. (a) The concentration of neutral particles above the membrane is higher than below which causes a downward net flow. (b) The concentration of the positively charged particles are the same on both sides of the membrane and, hence, there is no concentration gradient. Due to the potential difference over the membrane, however, there is an upward net flow of positively charged particles. (c) The concentration of particles is higher above the membrane than below which tends to push particles downwards. The positive charge of the particles in combination with the voltage gradient, however, tends to push particles upwards. For certain potential and concentration differences, these two effects cancel each other which results in a zero net flow.

At the *equilibrium potential* for a particular ion, the concentration and voltage gradients just balance and there is no net flow of that ion across the membrane. This potential is given by the *Nernst equation* that for a univalent ion at 20 °C is

$$V = 58 \log_{10} \frac{C_o}{C_i} \quad \text{[mV]}$$

where V is the equilibrium potential (internal minus external), and C_o and C_i are the outside and inside concentrations of the ion, respectively.

If we insert the concentrations found in the squid axon of the potassium (K^+), sodium (Na^+), and chloride (Cl^-) ions, we obtain the following equilibrium potentials [67, p. 44]

$$\begin{aligned} V_K &= -75\ mV \\ V_{Na} &= +55\ mV \\ V_{Cl} &\approx -65\ mV \ . \end{aligned}$$

Knowing that the axon's resting potential is about -65 mV, the following three things can be noted. First, the chloride ions are in equilibrium and no net flow over

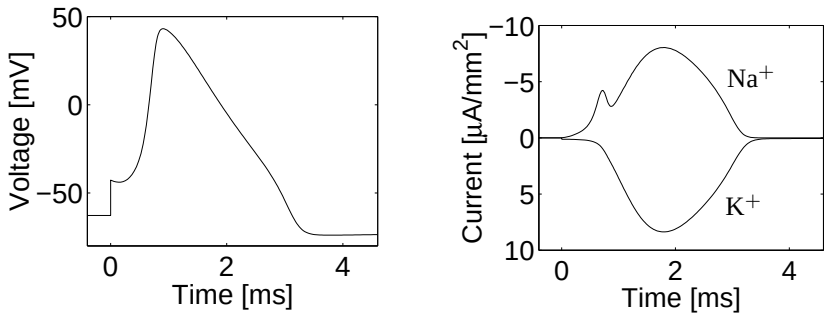

Figure 1.3: The change of the membrane potential and the ion currents during the conduction of an AP. (The current is defined to be positive if it flows out of the cell.) At $t = 0$, the membrane is depolarized by a current impulse that increases the membrane potential with $+20$ mV. (a) The depolarization causes a quick increase of the membrane potential to about $+50$ mV. This is followed by a slower reduction phase where the lowest point is actually below the initial, resting potential (hyperpolarization). (b) The depolarization causes an increased permeability to sodium ions (Na^+) which is manifested by a pronounced influx (negative current) of these ions because the concentration and voltage gradients both asserts a push into the cell. Above a certain membrane potential, voltage-gated potassium channels open which increases the permeability to potassium ions (K^+). This is manifested by an efflux (positive current) of these ions because the concentration and voltage gradients both assert a push out of the cell.

the membrane occurs. Second, there will be an *influx* of sodium ions according to its equilibrium potential being *above* the resting potential. Third, there will be an *efflux* of potassium ions according to its equilibrium potential being *below* the resting potential.

To balance these last two effects, the membrane contains *ion pumps* of which the most important one in this context is the Na^+/K^+ pump. Each "stroke" forces three sodium ions *out* of the cell and two potassium ions *into* the cell. Hence, the ion concentrations and thereby the membrane potential are kept at constant levels.

1.1.2 The Hodgkin-Huxley action potential

With the knowledge about the role of sodium, but without knowing about the ion channels which were discovered much later, Hodgkin and Huxley began a series of experiments where they tested different conditions and measured the resulting membrane potential.

After a tremendous amount of experimental work and manual calculations, they were in 1952 able to present a mathematical model of the depolarization of

the cell membrane. For this effort they received the Nobel prize in 1963 (shared with John C. Eccles).

Hodgkin and Huxley showed that upon depolarizing the cell membrane, the permeability to sodium suddenly increases which allows the voltage and concentration gradients to push sodium ions into the cell. The sodium influx increases the membrane potential in an effort to reach the equilibrium potential of the sodium ions (55 mV), see Figure. 1.3.

Before equilibrium is reached, however, the permeability to potassium increases which allows the voltage and concentration gradients to push potassium ions out of the cell. The potassium efflux counteracts the sodium influx which causes the membrane potential to peak around 50 mV and slowly decrease. Today, we know that these effects are excerted in *ion channels* that actively open and close according to a certain set of rules.

The depolarization also triggers the adjacent parts of the cell membrane, thus, causing it to spread and conduct along the fiber. The effect is very similar to when lining up dominos close to each other and tipping one of them over. The "depolarized" domino hits the neighboring domino and tips it over which causes the next one to do the same and so on until the last domino has fallen.

To be able to do this again, all dominos need to be erected and lined up. This is quite the same as in the nerve fiber where the ion channels and the ion concentration need to be restored before a new AP may be conducted, called *repolarization*.

The speed with which the AP propagate, the *conduction velocity*, is mainly dependent on the square root of the fiber diameter. In the case of the squid giant axon this means a conduction velocity of about 30 m/s; a quite remarkable value.

There is an evident trade-off here between transmission delay on one hand and "bulkiness" on the other. Since space is at premium for any organism, the enormous size of this axon betrays something about the *importance* of a short transmission delay in this case. A closer look would consequently disclose that this axon is part of the squid's jet-propulsion system; a quite reasonably function to prioritize considering the obvious drawbacks of becoming a prey.

1.1.3 Myelination

The propagation of the AP depends on the coordinated action of both the active current that flows through the voltage-dependent ion channels as well as the passive current that continuously flows through the cell membrane. As a consequence, the conduction velocity is determined by both these factors.

One way of improving the passive current flow is to increase the diameter of the axon because this reduces the internal resistance of the axon. The consequent increase in conduction velocity presumably explains why invertebrates such as the

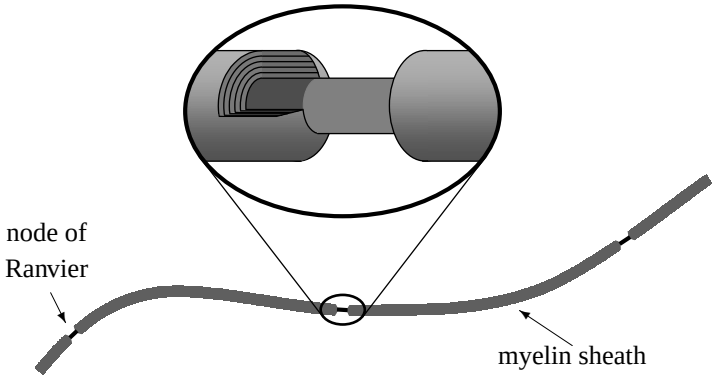

Figure 1.4: A myelinated nerve fiber where one Ranvier node is enlarged clearly showing the multiple layers of the myelin sheath around the cell membrane. At the nodes, the cell membrane is exposed to the extracellular medium which allows the AP to be regenerated.

squid has evolved giant axons.

Another way of improving the passive current flow is to insulate the axonal membrane because this effectively reduces the current leakage, thereby increasing the distance of passive current flow along the axon. In vertebrates, this strategy has resulted in *myelination* which is a more cost efficient solution to the delay/bulk trade-off than the increased-diameter approach.

With the myelination strategy, the time-consuming AP generation in an adjacent segment, denoted as *regeneration*, may be done at discrete points along the axon instead of more or less continuously. In principal, every regeneration takes a certain amount of time, so, by extending the distances between the regeneration points, the AP is forced to propagate in "jumps" and the conduction velocity is increased.

The regeneration takes place in between the insulated parts at the so-called *nodes of Ranvier* where the axon is exposed to extracellular medium, see Figure 1.4. The internode distance is a balance between conduction velocity and reliability; a longer distance yields increased velocity but decreased realiability of the regeneration. Typically, the nodes are separated by a distance corresponding to about a hundred axon diameters which results in conduction velocities ranging from 6 m/s to more than 130 m/s.[2]

Vertebrates thus have a rich variety of nerve fibers to choose from in order to find the best trade-off between transmission delay on one hand and the space occu-

[2] As a rule of thumb, the conduction velocity [m/s] is given by multiplying the fiber diameter [μm] with 6 [24, p. 72].

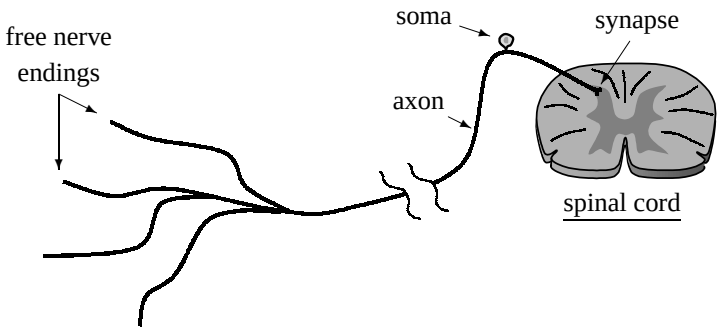

Figure 1.5: A nociceptor with the most important parts indicated.

pation on the other. What's best in the particular case depends on what information that is to be transmitted and the importance of a short transmission delay.

1.1.4 Sensory organs and receptors

Highly specialized nerve endings, called *receptors*, convert physical events into encoded messages that are passed on for further processing.

Using only five basic senses, somatic sensation (mechanical, thermal, or chemical stimuli), vision (photons), audition (sound waves), vestibular sensation (head movements), and chemical senses (taste/odour), we are able to get a good perception about our surrounding environment.

Presenting all these sensory systems would, however, be a daunting challenge. This presentation will therefore be limited to the somatic sensory system. In particular, only the receptors responsible for reporting temperature and painful stimuli will be discussed.

These receptors are called *nociceptors* (*noceo*, Latin: 'do harm') because they primarily detect noxious stimuli. Basically, the nociceptors are constituted by *free nerve endings*, see Figure 1.5, of either slowly conducting myelinated (Aδ) nerve fibers (about 20 m/s) or even slower unmyelinated (C) nerve fibers (less than 2 m/s).

Not surprisingly, the Aδ nociceptors respond to dangerously intense mechanical or mechanothermal stimuli that require an urgent response whereas, in general, the C nociceptors respond to less urgent sensations such as thermal, mechanical, or chemical stimuli.

An important discovery was the finding that nociception actually involves specialized neurons, not simply excessive discharges of the neurons that respond to normal stimulus intensities. Regardless of the discharge rate of non-nociceptors, the stimulus is normally not perceived as painful whereas, in contrast, already low

discharge rates of a population of nociceptors actually is.

There are two characteristics of nociceptors that also make them different from other sensors, namely: *sensitization*, and *modulation*. Sensitization is caused by tissue damage and the release of various substances that bring normally silent nociceptors into a sensitized state. The resulting phenomenon is *hyperalgesia* when even light touch could be painful. This may, for example, be experienced after being exposed to the sun for too long.

The modulation of pain is not completely understood but it is clear that neurons in the spinal cord have the ability to inhibit the relaying of the nociceptor APs to higher neurons and ultimately our consciousness. An everyday example of this is the ability to reduce the sensation of sharp pain by activating mechano receptors. For example, by gently blowing towards an injured site, the pain is relieved.

The perhaps most intriguing finding in this latter respect was the finding of endogeneous opioids (the endorphins belong to this family) and opiate sensitive regions in both the central and the peripheral nervous system. It was now clear that pain may be relieved in two independent ways: disabling the nociceptors ("silencing the source") and/or down-modulating the transmission ("cutting the wire").

1.2 Recording C-fiber APs

In order to further increase the knowledge of the functional properties of the C nociceptors, it was necessary to obtain recordings of the emitted APs. A task that was not easily accomplished.

First, the fibers are bundled together into *fascicles* with a thick insulating connective tissue, the *perineurium*, surrounding it, see Figure 1.6. Second, the fascicles are bundled together with blood vessels and enwrapped in a connective tissue sheath, the *epineurium*. Third, using a thin needle electrode, it is indeed possible to penetrate the nerve and position the electrode in a fascicle. APs from a large number of nerve fibers are recorded, however, and individual studies of the APs originating from a particular nerve fiber is difficult.

1.2.1 The marking phenomenon

To overcome this problem, Hallin and Torebjörk introduced a method that shows the excitation of a C-fiber by utilizing the so-called *marking phenomenon*. The phenomenon stems from the slight decrease of a fiber's conduction velocity after an AP has been conducted. The conduction velocity then slowly returns to its initial value.

The principle of the method is to apply an electrical impulse repetitively, at a

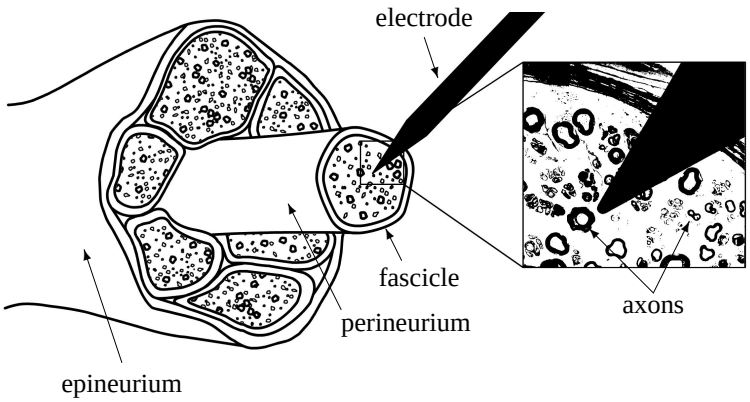

Figure 1.6: A needle electrode inserted into a nerve with the most important parts identified. As the enlargement shows, the electrode records from several fibers at the same time due to its large size compared to the nerve axons.

constant, low frequency (0.25 Hz), into the innervation territory of the C-fiber under study, see Figure 1.7. For each impulse, a single AP is evoked and appears in the recording after a certain latency. To document the response characteristics of the C-fiber, a physiological test stimulus (e.g., mechanical, temperature, or chemical) is applied into the receptive field of the fiber. If such a stimulus generates additional APs, the conduction velocity of the affected fiber decreases. The following APs excited by the repetitive stimuli thereby show a noticeable increase in latency.

This change in latency is used as a *marker* to indicate that the C-fiber responded to the applied physiological stimulus. In addition, the magnitude of the latency increase provides information about the number of APs that were generated by the test stimulus.

To enhance the efficiency of these experiments, a computer-supported recording system is used that both emits the repetitive stimuli and records the responses. Often, several fibers are activated and recorded simultaneously, but due to differences in conduction velocity of the individual C-fibers, the APs are spaced in time. Using the marking phenomenon, it is thus possible to discriminate and classify separate C-fibers by examining their characteristic latency responses.

1.2.2 Analyzing the signal

Previously, the analysis of the recorded traces was carried out manually which was very time consuming. To facilitate the analysis, a computer program that de-

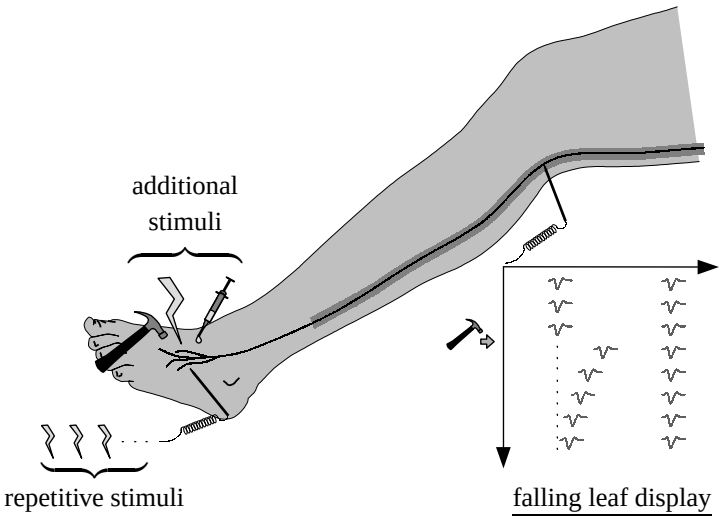

Figure 1.7: The recording setup. Repetitive, electrical impulses are delivered through a needle electrode inserted into the skin of the foot. Each triggered nerve fiber emits a single AP that is recorded at the knee via an electrode inserted into the corresponding nerve. In this case, there are two simultaneously active fibers which APs are recorded after a certain latency. The recorded APs for a particular triggering impulse are displayed from left to right in the falling leaf display. Successive responses are displayed in traces from top to bottom. To study the characteristics of a particular nerve fiber, an additional stimulus (e.g., mechanical, electrical, or chemical) is applied into the innervation area. The fibers responding to the additional stimulus are easily detected by their delayed response to the repetitive stimuli. In this case, the mechanical stimulus applied in between trace three and four triggered the first fiber as shown by its increased latency. Following this, the fiber recovers gradually as indicated by the APs returning to the latency prior to the activation (indicated by a dotted line). The right fiber did not respond to the mechanical stimulus and, hence, its latency was retained throughout the recording.

tects the APs, discriminates between APs originating from different C-fibers, and estimates latency shifts and recovery constants quantitatively was developed, see Figure 1.8. The most important aspects of the analysis are the detection and discrimination of the APs. Once this is accomplished, it is straight-forward to fit a parametrical model to the data in order to obtain the sought parameters.

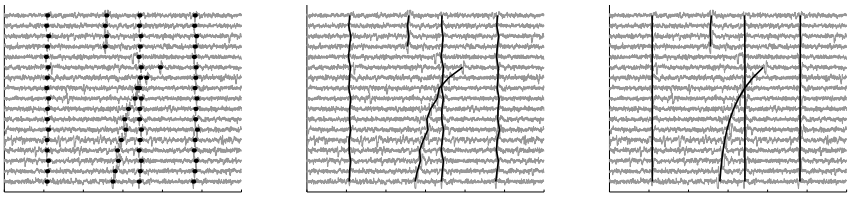

(a) (b) (c)

Figure 1.8: Sample results from the three-step analysis algorithm: (a) the detected APs, (b) the resulting five tracks after tracking, and (c) the final trajectories obtained by fitting an exponential function to the tracks.

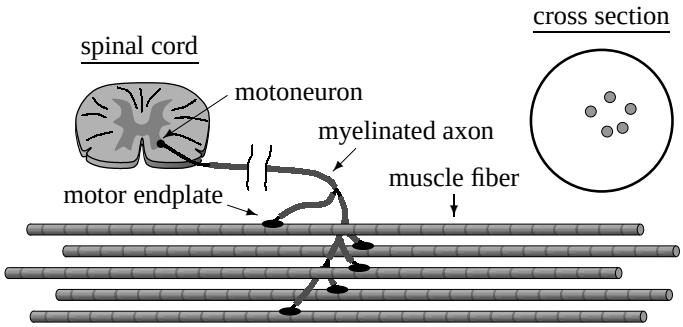

Figure 1.9: The motor unit consists of the motoneuron in the spinal cord, the myelinated axon, the motor endplate, and the innervated muscle fibers.

1.3 The constitution and function of muscles

As noted already by Galvani and Volta, a muscle contraction is initiated if the corresponding nerve is stimulated by an electrical impulse. Further experiments showed that the muscles actually shared many of the electrical characteristics of the nerves. It was discovered that the muscles too may be triggered by an electrical impulse and conduct an AP after being triggered. The latter was demonstrated by using a second frog leg as a detecting device and attaching its nerve to a muscle of the first leg.

1.3.1 The motor unit

Later anatomical studies also revealed that the muscles, similar to the nerves, are constituted by individual fibers where each fiber is a single cell. The muscle cell membranes also share most of the properties of the nerve cell membranes. The

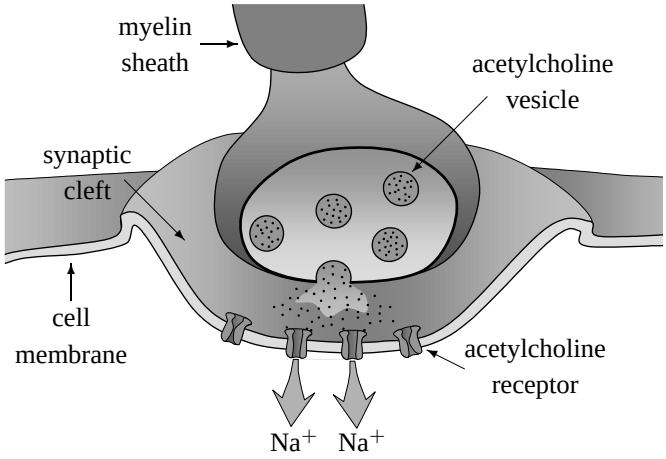

Figure 1.10: The neuromuscular junction, or motor endplate. When the AP arrives through the myelinated axon, it causes the vesicles to empty their acetylcholine molecules into the synaptic cleft. The neurotransmitter diffuses across the cleft and binds to the corresponding receptor. This activates the receptor and lets sodium ions (Na^+) pass through which depolarizes the cell membrane. If the depolarization is large enough, an AP is triggered.

results from the study of the squid giant axon are in general applicable to muscle fibers as well. To mention a few examples, the Hodgkin-Huxley model may be used to model muscle fiber APs and the conduction velocity of the muscle fibers increase with diameter as is the case for nerve fibers. In conclusion, what has been said above about the electrical characteristics of nerve fibers is in principal valid for muscle fibers as well.

The extension of the fibers differ, however. Muscle fibers are limited to the muscle whereas nerve fibers extends from a *motoneuron* in the spinal cord, via a peripheral nerve, all the way to the *innervated* muscle, see Figure 1.9.

The muscle is organized into functional groups of fibers each controlled by the same motoneuron. This constellation constitutes the smallest functional unit of the muscle and is called a *motor unit* (MU). With its axon, the motoneuron innervates its muscle fibers (typically a few hundred) via the *neuromuscular junction* (NMJ), called the *motor endplate*, one for each muscle fiber.

The different MUs are intermingeled with each other and have their muscle fibers randomly distributed. Thus, a particular fiber is in general surrounded by fibers belonging to other MUs.

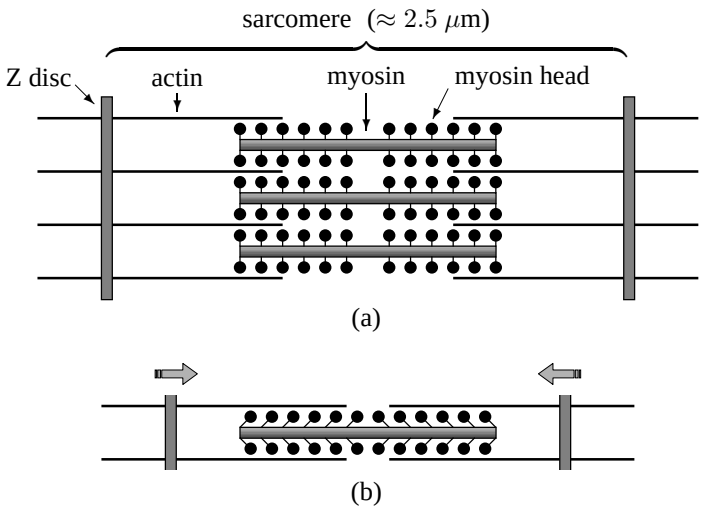

Figure 1.11: The principal constitution of the myofibrils that make up the bulk of the muscle fiber. (a) Each myofibril is made up of long chains of sarcomeres that are attached through the Z discs and consists of actin and myosin filaments. (b) During a contraction, the myosin heads adhere to the actin and undergo a conformational change that forces the Z discs together.

1.3.2 The motor endplate

In contrast to nerve and muscle fibers where the information is carried by electrical events, the APs, the motor endplate use chemical events, neurotransmitters, as information carriers.

Whenever an AP enters the synapse at the nerve terminal, the transmitter substance (acetylcholine) is released and diffuses across the *synaptic cleft* to receptors at the muscle fiber membrane, see Figure 1.10. When the transmitter binds to the receptors, sodium channels open and the cell membrane is depolarized, thereby initiating an AP.

Because of the construction of the motor endplate, there is a delay ($\approx$ 0.5 ms) associated with the arrival of the nerve impulse at the terminal and its further excitation of the muscle fiber. Moreover, this delay has a certain variability, the *jitter*, which is stochastic (standard deviation about 5-40 μs) and may change with disease. Hence, measuring the jitter is a valuable tool when studying the functional properties of the MU.

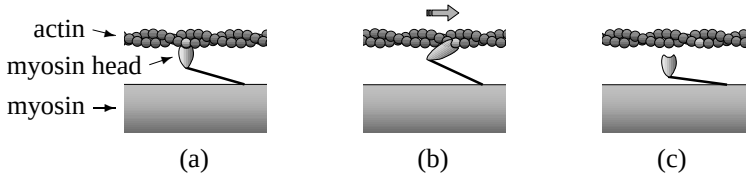

Figure 1.12: A detailed view of a contraction according to the sliding filament theory. (a) The myosin head bind to the actin. (b) The myosin undergoes a change in shape which forces the actin to the right (the power stroke). (c) Through an energy consuming process, the head is released from the actin and its shape is restored.

1.3.3 Muscle contraction

The depolarization of the muscle cell membrane initiates mechanical changes in the muscle fiber that makes it shorter through a minuscule machinery. The bulk of each muscle fiber constists of bundled *myofibrils* that are made up of *myosin* and *actin* filaments, see Figure 1.11. The filaments are organized into *sarcomeres*, separated by the *Z discs*, and work like a rack where the heads on the myosin filaments act as cogs that cling on to the actin filaments.

The conduction of the AP causes calcium (Ca^{2+}) to be released which, according to the sliding filament model, results in the following steps, see Figure 1.12:

1. The heads of the myosin bind to the actin filaments.
2. The heads are bended which causes a contraction by sliding the filaments past each other, the *power stroke*.
3. By consuming energy, the heads are detached and straightened.
4. The process is repeated as long as there are calcium and energy available.

Whenever the membrane potential returns to its resting level, the release of calcium ceases and the free calcium is quickly removed by efficient ion pumps. If this does not work for some reason, the muscle will be “stiff” and unable to relax. *Rigor Mortis* is the extreme of this situation. The free calcium causes the myosin to cling to the actin and contract but is unable to detach due to lack of energy. This condition remains until the filaments disintegrates in the decomposition process.

Due to the construction of the contraction machinery, a single AP causes a *twitch* in the muscle fibers of the corresponding MU that consists of a quick increase in muscle force followed by a somewhat slower return to zero, see Figure 1.13. By emitting a series of APs, the twitches summate to a smooth continuous contraction producing a higher and more sustained force. By activating other MUs as well, the muscle force may be increased even more.

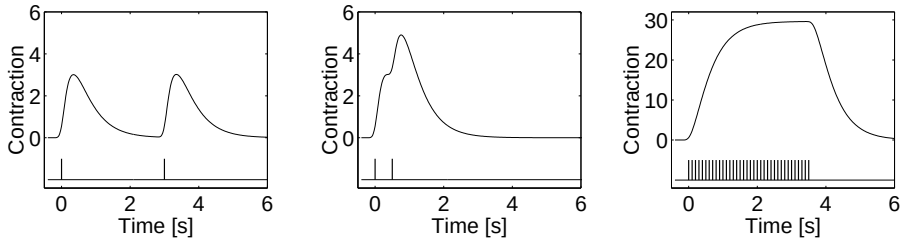

Figure 1.13: Each AP causes a quick increase in force excerted by the fibers within the MU followed by a slow relaxation. These twitches integrate into a contraction that is proportional to the triggering frequency. The diagrams show the contraction (arbitrary units) when (a) the APs are three seconds apart, (b) the APs are 0.5 s (2 Hz) apart, and (c) the APs are 0.1 s (10 Hz) apart. The times of arrival of the APs are indicated by vertical bars.

In each muscle, there are 100-500 MUs that are working in parallell to provide the correct muscle force. They are independently controlled by their individual motoneurons through frequency modulation and increasing muscle force is obtained by increasing the stimulation frequency of already active MUs and by recruitment of new ones.

1.4 The line source model

From the first evident demonstration of the electrical activity, the *electromyogram* (EMG), in contracting muscles, it has been clear that a good understanding of the underlying processes is vital in order to interpret the EMG correctly. Electromyography, in interplay with various anatomical techniques, has provided much of the present knowledge of the structural organization and the nervous control of muscle.

A vital tool in gaining this knowledge has been, and still is, modeling and simulation. A simple and yet reasonably accurate model is the *line source model* that is obtained by considering the AP as a convolution of a weighting function and a transmembrane current lumped to the center of the muscle fiber. The weighting function depends on the used recording electrode whereas the transmembrane current depends on the particular muscle fiber. The resulting EMG signal is then simply the sum of the contributions from all muscle fibers in the recorded muscle.

With the increased availability of digital computers, conducting simulations has been simplified considerably. Computerized simulations require, however, discrete-time models where the time axis consists of discrete points. This is different from the real world where the time is continuous

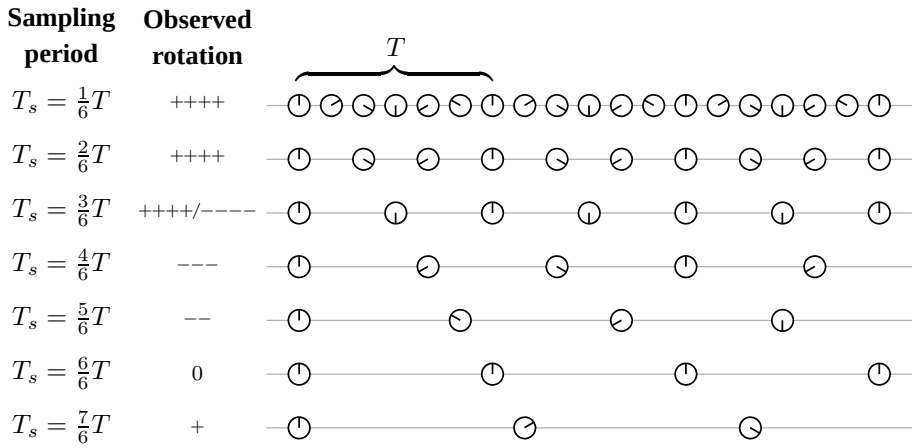

Figure 1.14: The importance of selecting an appropriate sampling period to avoid aliasing is illustrated using a rotating wheel. Unless the sampling period is short enough with respect to the period T, in which the wheel completes one full revolution, the samples constitute a "skewed" view of the continuous-time reality. In the figure, the observed direction of the rotation is indicated by '$+$' for clockwise (cw) rotation and '$-$' for counter-clockwise (ccw) rotation, respectively. The speed is symbolized by the number of repititions of the direction indicator ('0' for stationary rotation). As the figure shows, the correct direction and speed of rotation may be observed for sampling periods $T_s < \frac{1}{2}T$. For $T_s = \frac{1}{2}T$, the correct speed may indeed be observed, but the direction is ambiguous. Using longer sampling periods, the rotation observed in the samples no longer reflects the original rotation. Denoting the original rotating speed as very fast cw, the observed rotation pass through, in sequence, fast ccw, ccw, stationary, and slowly cw as the sampling period increases ($T_s > \frac{1}{2}T$). In these cases, the observed rotation is an "alias" of the original rotation; hence, the term aliasing for this type of distorsion.

1.4.1 Sampling and aliasing

The transformation, or *discretization*, from continuous time to discrete time is often referred to as *sampling* because the continuous-time model is sampled (measured) at discrete points in time. It is important that this is done sufficiently often to also catch the fastest changing characteristics. If not, the discrete-time representation become distorted through what is called *aliasing*. A good example of aliasing is in movie sequences with accelerating cars where the wheels (preferrable with spokes) are visible. First, the wheels (correctly) look like they are rotating faster and faster. Then, the rotation (falsely) looks like it rotates backwards or even stops. In this case, the sampling frequency (frame rate) is too low to catch the characteristics of

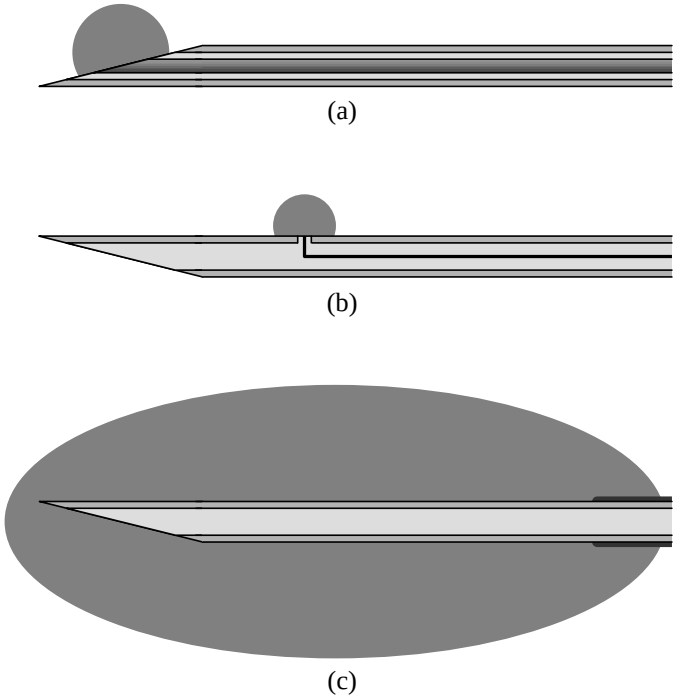

Figure 1.15: The three most common electrode types with their pick-up distance indicated: (a) the CN electrode, (b) the SF electrode, and (c) the Macro electrode.

the quickly rotating wheels.

Figure 1.14 shows this phenomenon from a little different perspective. Here, the rotational speed is constant but the sampling frequency is changed. However, the same observations as in the example above are illustrated.

Addressing the aliasing in the discretization process is an important issue. It can be done in two ways: either the discretization frequency is selected high enough with respect to the fastest changing characteristics, or these characterics are removed by prefiltering before the actual discretization. In the example above with the accelerating car, these alternatives correspond to either increasing the frame rate of the camera, or covering the wheels using smooth hub caps prior to the shooting.

1.4.2 Electrode types

The EMG signal may be acquired using either surface electrodes that are attached on the skin surface or, needle electrodes that are inserted transcutaneously into the muscle. In this thesis, only the three most common needle electrodes are regarded, see Figure 1.15: the *concentric needle* (CN) electrode, the *single fiber* (SF) elec-

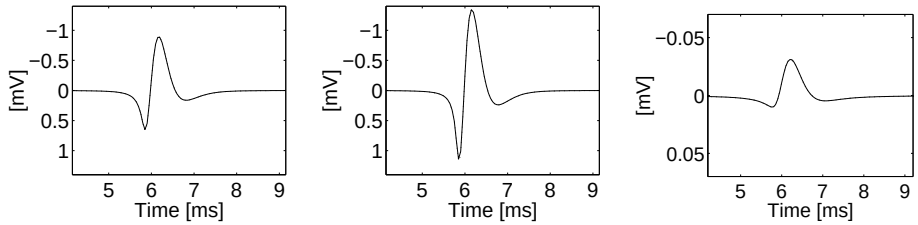

Figure 1.16: Examples of three APs as recorded with (a) the CN electrode, (b) the SF electrode, and (c) the Macro electrode, respectively. Note the different scale of the Macro AP.

trode, and the *Macro* electrode.

The CN electrode is a standard electrode used in clinical routine throughout the world. It has an elliptical recording area (150×580 μm) in the beveled tip of a steel cannula (diameter 0.45 mm). Often, the cannula is used as a reference electrode to obtain bipolar recordings. The electrode sums the electrical field from a number of muscle fibers in a given MU to obtain a *motor unit action potential* (MUAP). The shape of the MUAP reflects the number of muscle fibers, the synchronicity of their APs, and their concentration within the pick-up distance.

By using different electrodes, different resolutions can be obtained. For example, it is possible to record APs from individual muscle fibers using the *single fiber* (SF) electrode [86] [28]. This gives the possibility to study in detail some of the physiological characteristics involved in the generation of the EMG signal. Similarly, it is possible to record APs from entire MUs through the *Macro* electrode [79]. This electrode provides a broader view that, in some cases, is more suitable for diagnosis [71].

The SF electrode is constructed to selectively record APs from individual muscle fibers. The recording surface is a wire (diameter 25 μm) exposed at a side port of the electrode with the cannula as a reference. It is used to assess fiber density (FD) and to measure the jitter in the motor endplate.

The Macro electrode is the opposite of the SF electrode in that it records APs from the entire MU. Its recording area is the exposed tip (length 15 mm) of an insulated cannula with a distant electrode as a reference. This results in a broader view that may be used to estimate the total size of the MU and is in some cases more suitable for diagnosis than what is provided by the CN electrode.

1.4.3 Simulated APs

Using the line source model, fast and accurate simulations of different electrodes, muscle fibers, and electrode positions are readily obtained. As an example of this, Figure 1.16 shows three different APs as if recorded by the three most common electrode types. Note that the y axis increases downwards in line with the convention of displaying EMG signals.

The diameter of the simulated fiber was selected to 55 μm corresponding to a conduction velocity of 3.7 m/s. The electrodes were oriented perpendicular to the muscle fiber where the SF electrode and the CN electrode were positioned at a radial distance (center-to-center) of 100 μm.

The Macro electrode was positioned close to the fiber at a radial distance of 255 μm (a little more than the radius of the cannula plus the radius of the fiber).

1.5 The compound AP of the MU

By combining the line source model with knowledge about the constitution of the MU, compound APs of the MU is readily obtained.

First a MU is generated with a certain number of fibers having certain diameters and being distributed over a certain area, etc, in accordance with anatomical knowledge. The number of fibers present in a particular area is referred to as the *mean fiber concentration* (MFC).

Then, the insertion of the selected recording electrode is imagined. The "shuffling effect" of the beveled tip is simulated by moving the affected fibers to the upper side of the electrode, see Figure 1.17 (a).

Finally, the line source model is applied to each muscle fiber, taking the relative electrode position into account. The resulting individual APs are summed to obtain the compound AP of the MU for the particular electrode selected, see Figure 1.17 (b).

1.5.1 Changes in disease

The constitution and function of the MU may change in disease. The exact effect is of course individual for each disease depending on which category it represents; myopathies, neuropathies, or diseases in the neuromuscular junction.

Myopathies cause a loss or impairment of muscle fibers. In general the number of fibers within the MU decrease, but fibers may actually split longitudinally or regenerate in a compensatory process to meet the loss of fibers. Moreover, the fiber diameter variation is often found to be increased, with abnormally small and large muscle fibers.

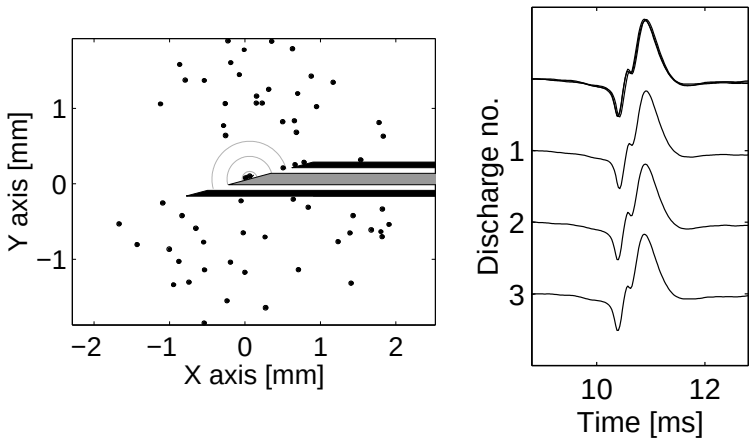

(a) (b)

Figure 1.17: Example of a simulated MUAP obtained with a concentric needle for a normal healthy muscle (MFC = 5 fibers/mm^2). (a) A cross section of the MU where the fibers and the electrode are shown. The semi circles indicate the distances 100, 300, and 500 μm, respectively. (b) The simulated MUAP for three discharges. On top, all discharges are drawn superimposed.

Neuropathies cause a loss of motoneurons or axons. In a compensatory process, surviving axons branch off and reinnervate the orphaned muscle fibers by *collateral sprouting*. Hence, the number of MUs decreases but their size in terms of number of fibers increases. Other findings may be a change in diameter of individual fibers and a temporarily increased jitter of recently reinnervated fibers.

Junctional diseases affect various key components that are vital for the function of the MU. If, e.g., the acetylcholine receptors in the motor endplate are reduced in number, the function of the muscle may be severely impaired. This may cause the variability of the synaptic delay, the jitter, to increase, or the triggering to sometimes fail; a condition called *blocking*.

As a rule of thumb, myopathies are manifested by small MUAPs and often the components of the MUAPs are “spread out” in time. Neuropathies are manifested by large MUAPs with multiple peaks corresponding to the increased number of fibers. The junctional diseases, finally, may often be diagnosed by the differences in the MUAP over time through studies of, e.g., the jitter and/or the blocking.

1.6 EMG analysis

Electromyography is today a common and efficient diagnostic tool that allows the clinician to follow changes in the neuromuscular system caused by disease pro-

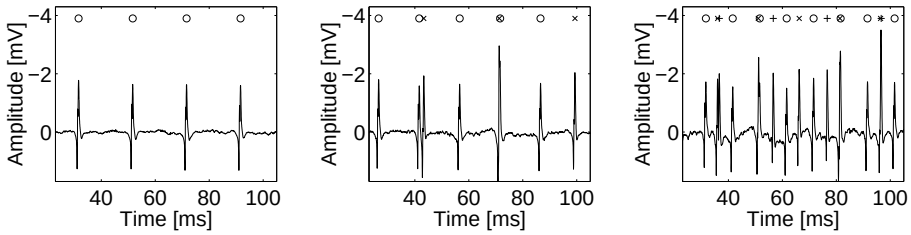

Figure 1.18: Intermingled MUAPs at various force levels with the firing frequency exaggerated for clarity. The number of recruited MUs in each diagram is (a) one, (b) two, and (c) three. The position of the peak is marked ($\circ \times +$) for each individual MUAP.

cesses.

The measured EMG signal is the summed contribution from all active muscle fibers within the entire muscle. Depending on the electrode, distant fibers contribute in a varying extent. The SF electrode, for example, effectively attenuates the contribution from distant fibers owing to the arrangement of the recording surface positioned within the reference.

The EMG signal is made up of the compound APs from each MU, see Figure 1.18. Because the muscle force is regulated by frequency modulation and recruitment/decruitment of MUs, the number of active MUs and their repetition frequency is varying with force level. Thus information regarding multiple MUs can be retrieved from a single EMG signal.

By *decomposing* the EMG signal and separating compound APs originating from different MUs, the analysis is often simplified. Each compound AP may then be analyzed separately which may include an effort to gain knowledge about the MU's constitution (e.g., through the MFC) or functional properties (e.g., through the jitter).

1.6.1 Analyzing the MUAPs

If possible, a complete decomposition of the MUAP into its constituent muscle fiber APs would add considerable information about normal and diseased MUs. The number of fibers within the pick-up distance of the electrode, for example, would be directly given by the number of AP components. Moreover, the jitter would be readily estimated through the variability in timing of the individual APs in subsequent discharges.

Deriving such an algorithm would be a daunting challenge, however. Perhaps is it even impossible unless sophisticated multichannel electrodes are adopted.

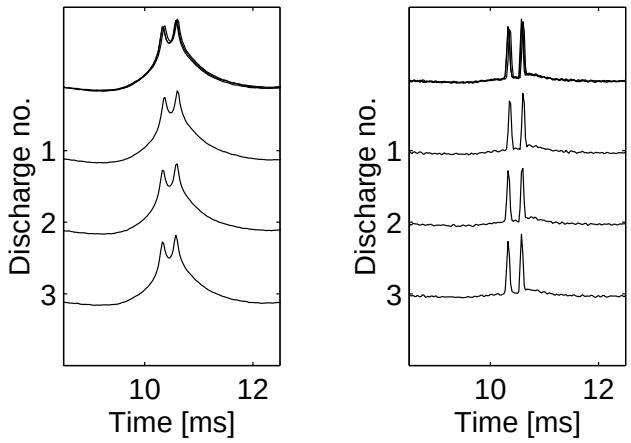

Figure 1.19: Example of applying the deconvoluting prefilters to three discharges of the MUAP in Figure 1.17 (b). (a) The partially deconvolved signal where each individual AP is monophasic. The diagram shows two active APs within the pick-up distance. (b) The fully deconvolved signal where each AP is transformed to a narrow impulse. In this signal, the two active APs are clearly visible. On top, all discharges are drawn superimposed.

Instead, a simpler approach is sought. To discriminate between myopathies and neuropathies, for example, it is sufficient to know the MFC which is directly proportional to the number of fibers within a certain radius (e.g., the pick-up distance).

A scaled version of this number works just as well and may be retrieved easily by assuring a direct relation between the number of fibers and some measurable quality of the analyzed signal. For example, knowing the amplitude of the compound AP would be sufficient in order to discriminate between myopathies and neuropathies if it was directly proportional to the number of fibers within the pick-up distance.

Normally, however, this is not the case because APs have positive and negative phases that make the sum unpredictable. This is called phase *canceling*. By prefiltering the compound AP with a filter that removes the multiphasic shape, a signal more suitable for diagnosis may be obtained, see Figure 1.19 (a). This signal is called the *partially deconvolved* MUAP because it removes the multiphasic shape only and keeps the “smearing” effect.

In the general case, the amplitude of the prefiltered compound AP is, however, not directly proportional to the number of fibers within the pick-up distance because the individual APs are distributed in time. Hence, the number of fibers may

be increased without affecting the amplitude.

A better measure in this respect might be the area because the area is always adding up regardless of the position in time. This requires that the signal being measured is monophasic.

To measure the jitter, there are two things to consider: the individual APs must be distinguishable, and neighboring APs must not disturb the localization. Both these requirements are met if the APs could be transformed into narrow impulses. Again, using a suitable prefilter this could be accomplished, see Figure 1.19 (b). This signal is called the *fully deconvolved* MUAP because it seeks to remove all the shaping of the APs while it keeps the amplitude and timing information.

1.7 Further reading

To obtain more information on many of the issues presented above the books listed below are good starting points.

- D. Purves, G. J. Augustine, D. Fitzpatrick, L. C. Katz, A.-S. LaMantia, and J. O. McNamara, *Neuroscience*, Sunderland, MA: Sinauer Associates, Inc., 1997

- E. R. Kandel and J. H. Schwartz, *Principles of Neural Science*, New York, NY: Elsevier North Holland, Inc., 1981

- S. Deutsch and A. Deutsch, *Understanding the Nervous System: An Engineering Perspective*, New York, NY: IEEE Press, 1993

- B. Alberts, D. Bray, J. Lewis, M. Raff, K. Roberts, and J. D. Watson *Molecular Biology of the Cell*, second edition, New York, NY: Garland Publishing, Inc., 1989

1.8 Objective of this thesis

The present thesis provides our perspective of the signal processing challenges arising in the neurophysiological field. The overall objective of this work is to develop methods that extract information from neural and muscular signals, not available by existing methods.

In particular, we address three principal categories within this field and refer to these as: *modeling*; *prefiltering and parameter assessment*; and *data detection and classification*. These are further presented below.

1.8.1 Modeling

Without doubt, the key tool in neurophysiology is the acquisition of signals and events that are used for diagnosis and research. A basic requirement is here the knowledge of the relationships that connect a certain signal property with a certain neurophysiological condition. As in virtually any other area, one efficient way in gaining this knowledge is by means of experiments followed by modeling and simulation.

The most important model presented herein is the modified line source model that models the recording of APs from a muscle fiber. The model has been implemented in a simulation program [83] that may contribute to new insights into the underlying processes of the generation of the EMG signal. This may in the longer perspective lead to improved diagnostic methods.

In a shorter perspective, this model can be used for research and educational purposes since it enables fast and accurate simulations of different anatomical conditions. Within a few seconds, the corresponding APs may be generated and visualized. Furthermore, benchmarks on different analysis algorithms may be carried out.

1.8.2 Prefiltering and parameter assessment

Within the daily routine, in particular, continual efforts are being made to make the examinations more efficient and to improve the reliability in diagnosis. Most of these efforts concern algorithms that are characterized by prefiltering (often using simple filters) followed by an assessment of the parameters to be used for diagnosis.

Based on a Wiener filter design, we present a more elaborate prefiltering method that strives at optimizing the filtered signal for the subsequent parameter assessment algorithm. Depending on the situation, the optimal prefilter will be different.

The current results from this approach indicate several advantages. First, the variability of the resulting parameter estimates decrease because the parameters are assessed using a signal that is more suitable for the task. Second, the need for different electrodes for examinations of various types may be reduced by applying specifically designed prefilters to enhance different features in the signal. Third, the Wiener filter design method provides a good intuitive coupling between the design variables and the properties of the resulting filter, which simplifies the tuning process.

1.8.3 Data detection and classification

When studying, e.g., the membrane properties of nerve C-fibers, APs originating from a specific C-fiber must be detected and identified. With the special record-

ing technique being used, the measured parameters form clusters in the parameter space. These clusters have (possibly) time-variant centroids, which effectively disqualify most clustering algorithms.

By considering the problem from a target tracking point of view, however, the APs originating from a particular C-fiber are tracked in subsequent responses to electrical stimulation. With this approach, an algorithm has been designed that has made the previously time-consuming, manual analysis much more efficient [57] [44].

This algorithm is a general implementation of a target tracker; only the tracking parameters and the predictor are coupled with the particular problem. Thus, this approach may be applied to virtually any problem where events occurring in multiple detections need to be classified.

1.9 Outline of the thesis

This thesis is divided into two major parts, *Methods* and *Applications*, respectively, of which the latter constitutes the main contribution.

Part I consists of Chapter 2-5 and is essentially a recapitulation of the most important methods used in the applications. These chapters have a disposition governed by the applications part, but are otherwise self-contained and may be read independently of each other.

In Chapter 2 an asynchronous matched filter (MF) detector needed for the application described in Chapter 9 is derived and analyzed. Because the assessment of important performance properties are crucial for the tuning of the algorithms in the applications chapter, this chapter provides the required framework that is then examplified on a hypothetical test signal.

Chapter 3 presents how a Kalman filter based on a continuous-time model is designed and tuned. Kalman filters are used by the multiple hypothesis tracking (MHT) algorithm, c. f. Chapter 4, where they provide predictions and assist in the track evaluation. Because it is important with good estimates in this regard, this chapter presents a consistency analysis procedure as well as an minimum mean squared error estimate of the initial values.

Chapter 4 provides a general description of multiple target tracking. Some common tracking algorithms are mentioned where the multiple hypothesis tracking (MHT) method receives most attention because it is used in the applications of Chapter 8 and Chapter 9.

Deconvolution using Wiener filters is the topic of Chapter 5 and this method is later used in Chapter 8 to filter and refine EMG signals. The implementation selected for this thesis is presented as well as an illustrative example.

The first chapter of Part II, Chapter 6, describes a modified line source model that can be used to simulate APs fast and accurately. The importance of avoiding aliasing when discretizing the model is stressed and the consequences of not doing so are shown through simulations. Moreover, through a simple transformation of the electrode specific weighting functions, a finite muscle fiber length is easily incorporated into the model.

In Chapter 7 represents a brief introduction to simulation of entire MUs. The anatomical and physiological assumptions and parameters used in this thesis are presented. Moreover, the changes in the MU induced by disease are mentioned and exemplified with cross sections and resulting compound APs of simulated MUs.

Chapter 8 explores the possibility to improve the assessment of muscle fiber concentration (MFC) and jitter by combining a MUAP obtained with a CN electrode with Wiener filter deconvolution, c. f. Chapter 5. The performance is compared both to a method currently used in clinical routine as well as to a recently proposed method for improving the jitter estimations. To discriminate between individual APs that originate from different muscle fibers, the MHT/Kalman tracking algorithm is used, c. f. Chapter 3 and Chapter 4.

Detection and classification of nerve APs is described in Chapter 9. The classification is implemented as a target tracking problem where the MHT/Kalman tracking method is used, c. f. Chapter 3 and Chapter 4. Examples on data obtained from real recordings are presented.

Chapter 10, finally, ends this thesis with some concluding remarks and presentation of possible work in the future.

1.9.1 Contributions of the author[3]

Chapter 9 was presented at

> Björn Hansson, Clemens Forster, and Erik Torebjörk, "Matched Filtering and Multiple Hypothesis Tracking Applied to C-fiber Action Potentials Recorded in Human Nerves," in *Proceedings of the SPIE Conference (AeroSense '98), Signal and Data Processing of Small Targets*, volume 3373, Orlando, FL, September 1998, pp. 582–593.

It is also described in

> Björn Hammarberg (Hansson), Clemens Forster, and Erik Torebjörk, "Parameter Estimation of Human Nerve C-Fibers using Matched Filtering and Multiple Hypothesis Tracking," *IEEE Transactions on Biomedical Engineering*, volume 49, no. 4, April 2002.

[3] When studying the author lists, it might be practical to know that, during the course of this work, the author got married and changed his last name from Hansson to Hammarberg.

The muscle fiber model in Chapter 6 is described in

> Björn Hammarberg (Hansson) and Erik Stålberg, "Insights into the Line Source Model for Improved Muscle Action Potential Modeling," submitted to *IEEE Transactions on Biomedical Engineering*.

The motor unit model of Chapter 7 in combination with the line source model is described in

> Lars Karlsson, Björn Hammarberg, and Erik Stålberg, "A Muscle Model to Study Electromyographic Signals," submitted to *Computer Methods and Programs in Biomedicine*.

The work in Chapter 8 will be presented in

> Björn Hammarberg, Mikael Sternad and Erik Stålberg, "A Wiener Filter Approach to Electromyography," in preparation.

In addition to the scientific work listed above, the author has contributed to the following papers that are connected to this thesis to a various degree:

- C. Weidner, M. Schmelz, R. Schmidt, B. Hansson, H. O. Handwerker, and H. E. Torebjörk, "Functional Attributes Discriminating Mechano-Insensitive and Mechano-Responsive C Nociceptors in Human Skin," *the Journal of Neuroscience*, volume 19, no. 22, pp. 10184–10190, November 1999.
- A. Sandberg, B. Hansson, and E. Stålberg, "Comparison between concentric needle EMG and macro EMG in patients with a history of polio," *Clinical Neurophysiology*, volume 110, no. 11, pp. 1900–1908, November 1999.
- C. Weidner, M. Schmelz, R. Schmidt, B. Hammarberg, K. Ørstavik, M. Hilliges, H. E. Torebjörk, and H. O. Handwerker, "Neural Signal Processing – the Underestimated Contribution of Peripheral Human C-fibers," submitted to *the Journal of Neuroscience*.

1.9.2 Financial support

We gratefully acknowledge the financial support obtained from the Swedish Medical Research Counsil (ES, 135) and (ET, 5206), the Deutsche Forschungsgemeinschaft (SFB 353), and a Max Planck Research Award to Prof. Erik Torebjörk.